Study Viscoelasticity of Ultrathin Poly(oligo(ethylene glycol) methacrylate) Brushes by a Quartz Crystal Microbalance with Dissipation

Long Fu, Xinan Chen, Jianan He, Chunyang Xiong, and Hongwei Ma*

Department of Biomedical Engineering, College of Engineering, Peking University, Beijing 100871, The People's Republic of China

Received November 23, 2007. Revised Manuscript Received March 14, 2008

Ultrathin polymer brushes play important roles in natural and artificial systems. To better understand and utilize their unique behaviors, characterization is a fundamental, but not trivial, task. In this paper, we demonstrated that the quartz crystal microbalance with dissipation (QCM-D) could be applied to study ultrathin poly(oligo(ethylene glycol) methacrylate) brushes. First, we identified four linear relations between dissipation/frequency changes and thickness changes, which were measured by QCM-D and ellipsometry, respectively. Next, we derived a set of equations starting from the Voigt model to further extract viscoelasticity of poly(OEGMA) brushes (≤30 nm) under high-frequency vibration in contact with water. The viscosity was $\sim 10^{-3}$ N s m^{-2} and the elasticity was $\sim 10^{5}$ N m^{-2}. Both were frequency dependent. Also discussed were other quantities such as the density (both the dry and wet film) and the working range of linear relations. These equations and quantitative information are important in advancing our understanding of ultrathin polymer brushes, which consequently promote our ability in designing functional surface coatings (i.e., in biosensor applications) and studying related interfacial phenomena.

Introduction

Ultrathin polymer brushes play important roles in natural and artificial systems, such as reducing friction[1] and nonspecific protein adsorption,[2] enhancing stability of colloids and supported lipid bilayers,[3,4] and altering the behavior of the nanofluid.[5] Characterization is the key to better understand and utilize their unique behaviors, but this is not a trivial task.[6–10] Here we demonstrated that when the quartz crystal microbalance with dissipation (QCM-D) was coupled with ellipsometry, this powerful, dual-probe instrument was useful in revealing the viscoelasticity and density of ultrathin polymer brushes under high-frequency vibration in contact with water, which could be described by the Voigt model (i.e., acoustic multilayer formalism).[11–14]

The physics behind a QCM is the piezoelectric phenomenon, and traditionally both the frequency and impedance changes are measured.[14–18] As a dual-probe instrument, QCM-D is able to measure both frequency and dissipation changes at multiple resonant modes in a single experiment with a temporal resolution down to 0.5 s.[19,20] Kasemo et al. applied QCM-D to study the process of lipid bilayer formation.[21] Höök et al. extensively studied the behavior of proteins at interfaces, such as the conformation changes of proteins after adsorption to a surface.[19,22] Two recent reports tried to obtain thin films' viscoelasticity via complex mathematical simulations.[4,23] Recently, we and other groups have applied QCM-D to monitor the process of surface-initiated polymerization (SIP),[20,24] but the dissipation factor was not analyzed. Quantitative analysis of QCM response was possible when a simple yet unexpected linear frequency−thickness ($f-t$) relation was discovered.[20] During the course of pursuing the origin of this $f-t$ relation, we realized that QCM-D combined with SIP was an excellent tool in revealing viscoelastic properties of ultrathin polymer brushes (≤30 nm).

Experimental Section

The initiator thiol (ω-mercaptoundecyl bromoisobutyrate) and QCM chips were received from HZDW (Hangzhou, China) as gifts. Monomer oligo(ethylene glycol) methacrylate, M_n = 475 (OEGMA475) was purchased from Aldrich.

SIP in QCM-D. The initiator thiol modified QCM chip was prepared as reported[20] and placed in a Q-Sense E4 sensor (Q-Sense, Gothenburg, Sweden). The activator generated by electron transfer (AGET) SIP was applied to grow polymer brushes.[20] Incomplete reaction mixture (IRM) was deoxygenated MilliQ water. Complete

* To whom correspondence should be addressed, hongwei@coe.pku.edu.cn.

(1) Raviv, U.; Giasson, S.; Kampf, N.; Gohy, J. F.; Jerome, R.; Klein, J. *Nature* **2003**, *425*, 163.
(2) Ma, H.; Hyun, J.; Stiller, P.; Chilkoti, A. *Adv. Mater.* **2004**, *16*, 338.
(3) Tanaka, M.; Sackmann, E. *Nature* **2005**, *437*, 656.
(4) Munro, J. C.; Frank, C. W. *Macromolecules* **2004**, *37*, 925.
(5) Atencia, J.; Beebe, D. J. *Nature* **2005**, *437*, 648.
(6) Milner, S. T. *Science* **1991**, *251*, 905.
(7) Zhao, B.; Brittain, W. J. *Prog. Polym. Sci.* **2000**, *25*, 677.
(8) Tsujii, Y.; Ohno, K.; Yamamoto, S.; Goto, A.; Fukuda, T. *Adv. Polym. Sci.* **2006**, *197*, 1.
(9) Priestley, R. D.; Ellison, C. J.; Broadbelt, L. J.; Torkelson, J. M. *Science* **2005**, *309*, 456.
(10) Muller, M. T.; Yan, X. P.; Lee, S. W.; Perry, S. S.; Spencer, N. D. *Macromolecules* **2005**, *38*, 3861.
(11) Rodahl, M.; Hook, F.; Krozer, A.; Brzezinski, P.; Kasemo, B. *Rev. Sci. Instrum.* **1995**, *66*, 3924.
(12) Voinova, M. V.; Rodahl, M.; Jonson, M.; Kasemo, B. *Phys. Scr.* **1999**, *59*, 391.
(13) Voinova, M. V.; Jonson, M.; Kasemo, B. *Biosens. Bioelectron.* **2002**, *17*, 835.
(14) Domack, A.; Prucker, O.; Ruhe, J.; Johannsmann, D. *Phys. Rev. E* **1997**, *56*(1), 680–689.
(15) Ward, M. D.; Buttry, D. A. *Science* **1990**, *249*, 1000.
(16) Johannsmann, D.; Mathauer, K.; Wegner, G.; Knoll, W. *Phys. Rev. B* **1992**, *46*(12), 7808–7815.
(17) Johannsmann, D. *J. Appl. Phys.* **2001**, *89*(11), 6356–6364.
(18) Brass, D. A.; Shull, K. R. *Langmuir* **2006**, *22*(22), 9225–9233.
(19) Hook, F.; Kasemo, B.; Nylander, T.; Fant, C.; Sott, K.; Elwing, H. *Anal. Chem.* **2001**, *73*, 5796.
(20) He, J.; Wu, Y. Z.; Wu, J.; Mao, X.; Fu, L.; Qian, T. C.; Fang, J.; Xiong, C. Y.; Xie, J. L.; Ma, H. W. *Macromolecules* **2007**, *40*, 3090.
(21) Keller, C. A.; Glasmastar, K.; Zhdanov, V. P.; Kasemo, B. *Phys. Rev. Lett.* **2000**, *84*, 5443.
(22) Hook, F.; Rodahl, M.; Kasemo, B.; Brzezinski, P. *Proc. Natl. Acad. Sci. U.S.A.* **1998**, *95*, 12271.
(23) Dutta, A. K.; Belfort, G. *Langmuir* **2007**, *23*, 3088.
(24) Cheng, N.; Azzaroni, O.; Moya, S.; Huck, W. T. S. *Macromol. Rapid Commun.* **2006**, *27*, 1632.

10.1021/la703661z CCC: $40.75
Published on Web 05/16/2008

Scheme 1. Experimental Design[a]

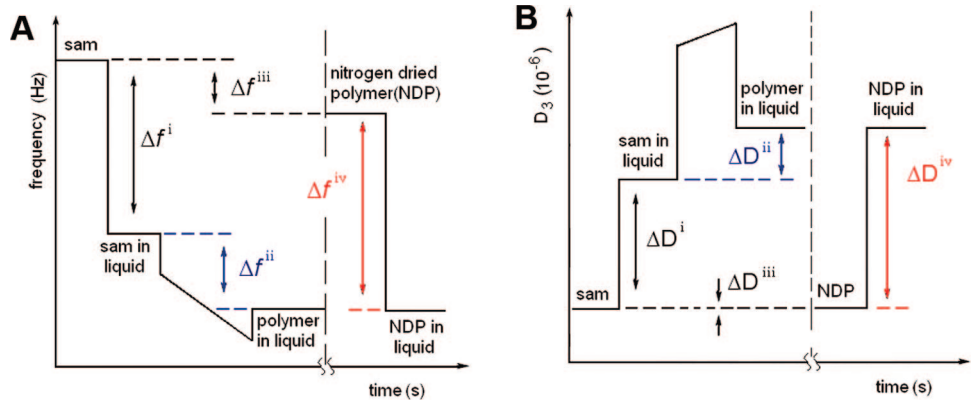

[a] SIP was conducted from an initiator-functionalized QCM chip in a QCM-D, which simultaneously measured (A) frequency and (B) dissipation changes throughout the SIP process, which resulted in a polymer brush coated QCM chip in contact with a liquid. Indicated are the definitions of Δf and ΔD (see text for details).

reaction mixture (CRM) was prepared by mixing well two parts. Part 1 was prepared by adding a specified amount of $CuCl_2$/Bipy (1:2 mol ratio) and a fixed amount of monomer to 5 mL of MilliQ water. Part 2 was prepared by adding a specified amount of ascorbic acid (AscA) to 5 mL of MilliQ water. After deoxygenation, the two parts were mixed together resulting in CRM, which had a mole ratio of monomer/$CuCl_2$/Bipy/AscA = 200/1/2/1, with a feed [$CuCl_2$] of 2.76 mM.

The QCM-D was first primed with IRM until a stable baseline was established. Polymerization was initiated by pumping the CRM mixture to the sensor cell at a speed of 70 mL h^{-1} (1−2 min) and reduced to ~3 mL h^{-1} after complete exchange of IRM with CRM (indicated by color change from colorless to red). SIP was continued for a specified time (30−600 min) at ~25 °C and monitored by QCM-D in real time. The polymerization was stopped by replacing CRM with IRM and rinsed with IRM until a stable baseline was reached. Samples were finally pulled out of the sensor cell and rinsed with methanol and MilliQ water and dried under flowing nitrogen before ellipsometry measurement.

Ellipsometry. Film thickness was measured on a M-2000V spectroscopic ellipsometer (J. A. Woollam Co., Inc.) at angles of 65, 70, and 75° and wavelengths from 500 to 800 nm. Ellipsometric data were fitted for the thickness with material-specific models, i.e., SAMs and poly(OEGMA) films with fixed (An, Bn) values of (1.45, 0.01) and (1.46, 0.01), respectively, using a Cauchy layer model. The ellipsometric thickness for each sample was independently measured at six different locations and is reported as the average ± standard error. For wet thickness, the measurement was conducted in a liquid cell at an angle of 70° and wavelengths from 500 to 800 nm and fitted for both thickness and optical properties.

Results and Discussion

Experimental Design and Empirical Equations. We carefully designed experiments (Scheme 1 and Figure 1) to separate the frequency and dissipation changes for theoretical analysis.

In a typical run, an initiator-functionalized QCM chip was first loaded to a QCM-D sensor so that its absolute resonating frequency could be measured. Second, IRM was pumped over the QCM chip to establish the baseline before polymerization, resulting in the first frequency and dissipation change, denoted as Δf^{i} and ΔD^{i}, respectively. Third, CRM was introduced to initiate polymerization. Polymer brushes were deposited on the QCM chip as a result of the in situ SIP, which led to the simultaneous decrease of frequency and increase of dissipation. After a certain period of time, IRM was pumped over the QCM chip again to quench SIP and establish the baseline after polymerization, resulting in Δf^{ii} and ΔD^{ii}. The QCM chip, now coated with polymers, was removed from the sensor, dried under nitrogen gas flow, and measured for film thickness by ellipsometry. Finally, the same QCM chip was reloaded to the QCM-D sensor and oscillated at air for establishing a baseline, then oscillated in IRM for a baseline in liquid, resulting in Δf^{iii} and ΔD^{iii}, Δf^{iv}, and ΔD^{iv}, respectively. Errors due to operations were minimized by careful experimental design (see Figures S1 and S2 and Table S1 in the Supporting Information).

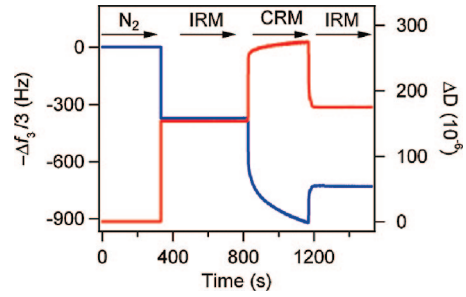

Figure 1. Representative QCM-D curves: IRM, incomplete reaction mixture; CRM, complete reaction mixture. The blue curve represents the frequency change and the red curve the dissipation change (overtone number $n = 3$) for a ~20 nm poly(OEGMA) brush.

We further defined

$$\Delta f^{v} = \Delta f^{iv} - \Delta f^{i} \quad (1)$$

$$\Delta D^{v} = \Delta D^{iv} - \Delta D^{i} \quad (2)$$

Oligo(ethylene glycol) methacrylate (OEGMA) was chosen as the model monomer because we were interested in its demonstrated biomedical applications.[2] The initiator density on QCM chips was varied via a binary mixed self-assembled monolayer technique. Three densities were tested, namely, 1.00, 0.42, and 0.15 (surface density as determined by X-ray photoelectron spectroscopy).[20] For all the figures in this paper, we applied the dry film thickness instead of the wet film thickness for the following two reasons: (i) We found that the ratio ($R = t_{f,wet}/t_{f,dry}$) was a constant for poly(OEGMA) brushes of different thickness but the same density, where $t_{f,dry}$ and $t_{f,wet}$ are the thickness of poly(OEGMA) in the dry state and in contact with water, respectively. In Figure 2, the value of R was found to be ~2 and the fitted A_n values were close to the reported value.[25] (ii) Practically, measurement of dry film thickness is more feasible than the measurement of wet film thickness.

(25) Bilen, B.; Skarlatos, Y.; Aktas, G.; Inci, M. N.; Dispinar, T.; Kose, M. M.; Sanyal, A., *J. Appl. Phys.* **2007**, *102*, (7).

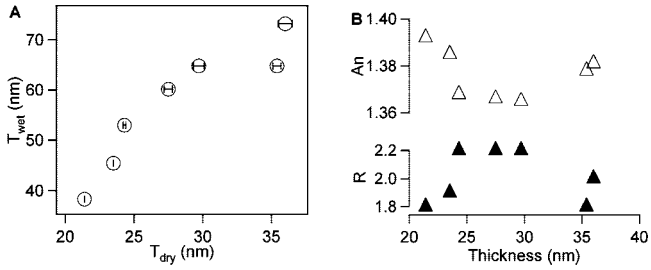

Figure 2. Film thickness of poly(OEGMA) determined by ellipsometry. The dry film thickness (T_{dry}) was measured in the air−solid mode and fitted with a fixed A_n value at 1.46. The wet thickness (T_{wet}) was measured in a liquid cell and fitted with a variable A_n (indicated in the upper Y axis of (B)). (A) T_{wet} plotted against T_{dry}. (B) The ratio ($R = t_{f,wet}/t_{f,dry}$) was plotted against $t_{f,dry}$, $R \approx 2$.

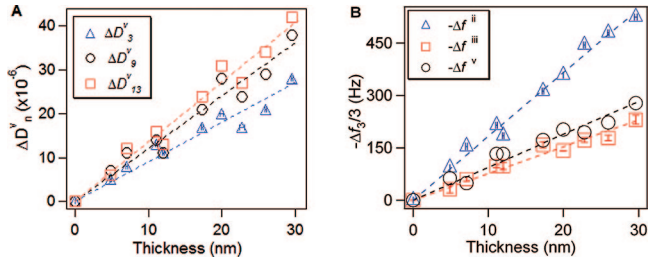

Figure 3. Linear relations between dissipation/frequency changes and thickness changes. Poly(OEGMA) brushes were grown from QCM chips of 1.00 initiator density. (A) ΔD_n^v showed a strong dependence on $t_{f,dry}$ (for clarity, only shown linear fit for three overtones, $k_{D,n,a}$ was the slope). (B) Frequency changes also showed a strong dependence on $t_{f,dry}$ (for clarity, only shown linear fit for $n = 3$). The R^2 values for linear fits were >0.94.

When the frequency and dissipation changes were plotted against dry film thickness (Figure 3 and Figure S4), we identified the following simple linear relations

$$\Delta D_n = k_{D,n,a} t_{f,dry} \tag{3}$$

$$-\frac{\Delta f_n^{ii}}{n} = k_{1,n,a} t_{f,dry} \tag{4}$$

$$-\frac{\Delta f_n^{iii}}{n} = k_{2,dry} t_{f,dry} \tag{5}$$

$$-\frac{\Delta f_n^{v}}{n} = k_{3,n,a} t_{f,dry} \tag{6}$$

In Figure 3, ΔD_n^v and Δf were found to have linear fits against $t_{f,dry}$, which led us to assume that the viscoelasticity was thickness independent (0−30 nm). It was obvious from Figure 4 that the dissipation changes were more sensitive at higher overtone numbers, and the frequency changes were more sensitive at lower overtone numbers. That is, the $k_{D,n,a}$ increased monotonically as the n increased while the $k_{1,n,a}$ and $k_{3,n,a}$ decreased monotonically as the n increased. And QCM-D was responsive to the change of initiator density: k values changed as the initiator density was varied from 1.00 to 0.15. We will come back to these points later. Thus, through carefully designed QCM-D experiments, we identified four empirical equations. The key was then to find the physical meaning of these equations.

Deduction of Theoretical Equations and Calculations. For a polymer-coated quartz chip vibrating in a liquid environment, the following equations were developed based on a continuum mechanics approach[12–14]

$$\Delta f \approx -\frac{1}{2\pi\rho_q t_q}\left[\frac{\eta_L}{\delta_L} + t_{f,wet}\rho_{f,wet}\omega - 2t_{f,wet}\left(\frac{\eta_L}{\delta_L}\right)^2 \frac{\eta_f\omega^2}{\mu_f + \eta_f\omega^2}\right] \tag{7}$$

$$\Delta D \approx \frac{1}{\pi\rho_q t_q f}\left[\frac{\eta_L}{\delta_L} + 2t_{f,wet}\left(\frac{\eta_L}{\delta_L}\right)^2 \frac{\mu_f\omega}{\mu_f + \eta_f\omega^2}\right] \tag{8}$$

$$\delta = \sqrt{\frac{2\eta}{\rho\omega}} \tag{9}$$

where the subscript q represents quartz, f represents the deposited film, and L is for liquid (water in this paper), μ_f is the elasticity and η_f is the viscosity, δ is the viscous penetration depth, t represents the film thickness, n is the overtone number, f is the resonating frequency, and ω is the angular excitation frequency.

Starting from this simplified model, we will first resolve the viscoelasticity of poly(OEGMA) from the dissipation changes because the three components of ΔD were experimentally determined (Scheme 1B). We will then extract mass related information from the frequency changes.

Viscoelasticity. Consider a QCM-D operating at seven frequencies ($f = 4.98n$ MHz, $n = 3$, 5, 7, 9, 11, and 13)

$$f_{q,n} = \frac{n v_q}{2t_q} \tag{10}$$

$$f_{q,n} = n f_{q,1} \tag{11}$$

$$\omega_{q,n} = 2\pi f_{q,n} \tag{12}$$

Substituting eqs 10–12 to eq 8, we rewrote eq 8 to the following format:

$$\Delta D_n \approx \frac{2}{n\pi\rho_q v_q}\left[\sqrt{\pi\eta_L\rho_L f_{q,n}} + \frac{\eta_L\rho_L\mu_f}{\left(\frac{\mu_f}{2\pi f_{q,n}}\right)^2 + \eta_f} t_{f,wet}\right] \tag{13}$$

Let:

$$\Delta D_n = \Delta D_{L,n} + \Delta D_{f,n} + \Delta D_{f,L,n} \tag{14}$$

The overall dissipation difference (ΔD_n) was due to the change from a bare QCM vibrating in air to a polymer brush coated QCM vibrating in liquid. This physical process can be treated as the sum of dissipation differences of three independent physical

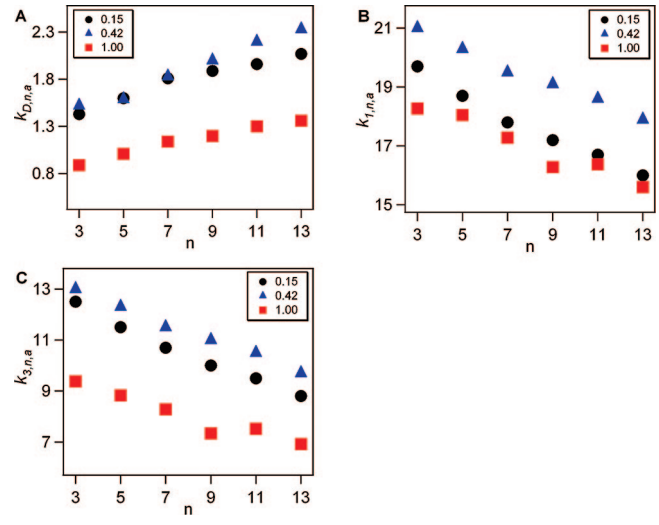

Figure 4. The values of k were n dependent except $k_{2,dry}$. Poly(OEGMA) brushes were grown from QCM chips of 1.00, 0.42, and 0.15 initiator densities. (A) $k_{D,n,a}$, (B) $k_{1,n,a}$, and (C) $k_{3,n,a}$.

processes: (i) from a bare QCM vibrating in air to vibrating in a liquid ($\Delta D_{L,n}$), from a bare QCM to a polymer-coated QCM vibrating in a liquid (ii) due to mass increase ($\Delta D_{f,n}$) and (iii) due to viscoelastic damping ($\Delta D_{f,L,n}$). From the experimental design (Scheme 1B), we have (i) $\Delta D_n^{i} = \Delta D_{L,n}$, which was a constant (see Figure S3), (ii) $\Delta D_n^{ii} = \Delta D_{f,n} + \Delta D_{f,L,n}$ and (iii) $\Delta D_n^{iii} = \Delta D_{f,n} = 0$ (because QCM-D was not sensitive enough to detect the dissipation change induced by the dry film). Consequently, we have $\Delta D_n^{ii} = \Delta D_n^{v}$ (from Scheme 1B), where a superscript (for example i, ii, iii, iv, and v) indicated an experimental data and a subscript (for example L and f) indicated theoretical data. We also have $f_{q,1} = 4.98$ MHz, $v_q = 3340$ m s^{-1}, $\rho_q = 2650$ kg m^{-3}, $\rho_L = 1000$ kg m^{-3}, $\eta_L = 8.9 \times 10^{-4}$ N s m^{-2}, and $t_{f,wet}$ has the unit 10^{-9} m. Substituting these constants into the above equations, one has

$$\Delta D_n = \Delta D_{L,n} = \frac{2}{n\pi\rho_q v_q}\sqrt{\pi\eta_L\rho_L f_{q,n}} = \frac{268.5}{\sqrt{n}} \quad (15)$$

$$\Delta D_{f,n} \cong 0 \quad (16)$$

$$\Delta D_n = \Delta D_{f,L,n} = \frac{6.4\times10^{-11}}{n}\frac{\mu_f}{\left(\frac{\mu_f}{2\pi f_{q,1}}\right)^2\left(\frac{1}{n}\right)^2 + \eta_f}t_{f,wet} \quad (17)$$

Equation 15 indicated the dissipation change induced by water addition was n dependent. Equation 16 was added so that eq 14 has the same format as that of eq 27 (see below). Substituting empirical eq 3 and $R = t_{f,wet}/t_{f,dry} = 2$ into eq 17, we have

$$\frac{2}{k_{D,n,a}} = \frac{1}{6.4\times10^{-11}}\left(\frac{1}{2\pi f_{q,1}}\right)^2\frac{\mu_f}{n} + \frac{\eta_f}{(6.4\times10^{-11})\mu_f}n \quad (18)$$

For simplicity, we assumed the viscosity and elasticity were n dependent as defined by eqs 19 and 20

$$\mu_f = \mu_0 n^{e} \quad (19)$$

$$\eta_f = \eta_0 n^{v} \quad (20)$$

where η_0 and μ_0 are the viscosity and elasticity at $n = 1$ (fundamental frequency).

Inserting eqs 19 and 20 to eq 18, we have the following equations for viscoelasticity calculation

$$\frac{1}{k_{D,n,a}} = an^{c} + bn^{d} \quad (21)$$

$$a = \frac{\mu_0}{1.26\times10^{5}} \quad (22)$$

$$b = \frac{\eta_0}{(1.28\times10^{-10})\mu_0} \quad (23)$$

$$c = e - 1 \quad (24)$$

$$d = 2v - e + 1 \quad (25)$$

From Figure 5A, we identified the values of a, b, c, and d in eq 21 (Table 1). It was interesting to notice that $a = b$ and $c = d$. At this stage, we could not exclude the possibility that there was a strong correlation among these parameters. In a different analysis, we assumed the viscosity and elasticity were independent of n (i.e., frequency) yet obtained similar viscosity and elasticity values: viscosity at 10^{-3} N s m^{-2} and elasticity at 10^{5} N m^{-2} (1 N m^{-2} = 1 Pa, see Figure S6 and Table S2). We have also applied free software (http://home.tu-clausthal.de/~pcdj/QCM_Modeling_QTM.zip) to model the viscoelasticity. A physically meaningful fit was obtained when the thickness was allowed to vary, which gave an acoustic thickness at 80 nm, 2-fold larger (i.e., $R = 4$) than the optical thickness measured by ellipsometry (personal communication with Dr. Johannsmann). This difference in acoustic thickness and optical thickness was critical in determining the density of wet film (see discussion later). From Table 1, we also noticed that the initiator density had a minor impact on the calculated viscoelasticity, which could be from two contradictory causes: (i) different initiator densities led to polymer brushes of different structures and properties but the QCM-D had limited sensitivity in discerning these slight changes or (ii) different initiator densities did not led to significant structural differences of the resulting polymer brushes because of the initiator efficiency (IE).[8] In the general field of SIP, there is a long-standing problem in determining the IE: a 1.00 initiator density with 10% IE is virtually the same as a 0.15 initiator density with 70% IE. To fully address this issue, which is an undergoing project in this laboratory, will require a separate paper.

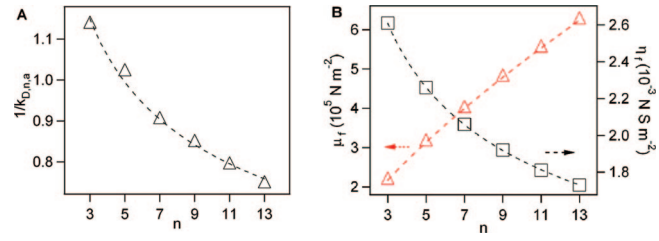

Figure 5. Dissipation changes revealed viscoelasticity. (A) the value of $1/k_{D,n,a}$ (1.00 initiator density) was plotted against n and fitted according eq 21, resulting in a good fit ($R^2 = 0.999$). (B) The viscosity and elasticity were calculated according eqs 19 and 20 using values from (A); see Table 1. See Figure S5 for 0.42 and 0.15 initiator densities.

Table 1. List of Fitted Values and Viscoelastic Properties for poly(OEGMA) at Different Initiator Densities[a]

initiator density	$an^c + bn^d$	η_f (N s m^{-2})	μ_f (N m^{-2})
1.00	$0.79n^{-0.28} + 0.79n^{-0.28}$	$3.2 \times 10^{-3}n^{-0.28}$	$9.8 \times 10^{4}n^{0.72}$
0.42	$0.49n^{-0.31} + 0.49n^{-0.31}$	$2.0 \times 10^{-3}n^{-0.31}$	$6.2 \times 10^{4}n^{0.69}$
0.15	$0.46n^{-0.26} + 0.46n^{-0.26}$	$1.8 \times 10^{-3}n^{-0.26}$	$5.8 \times 10^{4}n^{0.74}$

[a] n is the overtone number, 3, 5, 7, 9, 11, and 13.

Table 2. List of calculated density values for poly(OEGMA) at different initiator densities

initiator density	$k_{2,dry}$[a]	$\rho_{f,dry}$ (kg m^{-3})[b]	$\rho_{f,wet}$ (kg m^{-3})[c]
1.00	7.64	1364	1770
0.42	6.60	1179	2140
0.15	7.15	1277	1980

[a] The $k_{2,dry}$ values were from Figure 3A and Figure S7. [b] Calculated according eq 36. [c] Calculated according eq 37 and averaged from the six values (see Figure 6).

Mass and Density. Similarly, one could rearrange eq 7 to have the following form

$$\Delta f_n \approx -\frac{f_{q,1}}{\pi\rho_q v_q}\left[\sqrt{\pi\eta_L\rho_L f_{q,n}} + 2\pi f_{q,n}\rho_{f,wet}t_{f,wet} - \eta_L\rho_L\frac{2\pi\eta_f f_{q,n}}{\left(\frac{\mu_f}{2\pi f_{q,n}}\right)^2 + \eta_f}t_{f,wet}\right] \quad (26)$$

Let

$$\Delta f_n = \Delta f_{L,n} + \Delta f_{f,n} + \Delta f_{f,L,n} \quad (27)$$

$$\Delta f_{L,n} = -\frac{f_{q,1}}{\pi\rho_q v_q}\sqrt{\pi\eta_L\rho_L f_{q,n}} = -\frac{{f_{q,1}}^{3/2}}{\rho_q v_q}\sqrt{\frac{\eta_L\rho_L}{\pi}}\sqrt{n} \quad (28)$$

$$\Delta f_{f,n} = -\frac{f_{q,1}}{\pi\rho_q v_q}2\pi f_{q,n}\rho_{f,wet}t_{f,wet} = -\frac{2n{f_{q,1}}^2}{\rho_q v_q}\rho_{f,wet}t_{f,wet} \quad (29)$$

$$\Delta f_{f,L,n} = \frac{2{f_{q,1}}^2\eta_L\rho_L\eta_f}{\rho_q v_q}\frac{n}{\left(\frac{\mu_f}{2\pi f_{q,1}}\right)^2\left(\frac{1}{n}\right)^2 + \eta_f}t_{f,wet} \quad (30)$$

where subscript (f,L) stands for film in liquid.

The three frequency differences were analogous to that of dissipation changes: (i) from a bare QCM vibrating in air to vibrating in liquid ($\Delta f_{L,n}$), from a bare QCM to a polymer coated QCM vibrating in liquid (ii) due to mass increase ($\Delta f_{f,n}$) and (iii) due to viscoelastic damping ($\Delta f_{f,L,n}$). From the experimental design, we have (i) ${\Delta f_n}^{i} = \Delta f_{L,n}$, (ii) ${\Delta f_n}^{ii} = \Delta f_{f,n} + \Delta f_{f,L,n}$, and (iii) ${\Delta f_n}^{iii} = \Delta f_{f,n}$. Substituting the constants such as $f_{q,1}$, v_q, ρ_q, ρ_L, and η_L (L is water) and $t_{f,wet}$ has the unit of 10^{-9} m, we have

$$-\frac{\Delta f_{L,n}}{n} = \frac{668.5}{\sqrt{n}} \quad (31)$$

$$-\frac{\Delta f_{f,n}}{n} = 5.60\times10^{-3}\rho_{f,wet}t_{f,wet} = k_{2,n}t_{f,wet} \quad (32)$$

$$\frac{\Delta f_{f,L,n}}{n} = (4.99\times10^{-3})\eta_f\frac{1}{\left(\frac{\mu_f}{2\pi f_{q,1}}\right)^2\left(\frac{1}{n}\right)^2 + \eta_f}t_{f,wet} = k_{3,n}t_{f,wet} \quad (33)$$

Equation 31 indicated that the frequency change induced by water addition was a constant for different QCM chips but the same overtone number. Equation 32 was similar to eq 5: the former for wet film and the later for dry film. Both $k_{2,n}$ and $k_{3,n}$ were theoretical values and could not be directly determined by experiments.

Viscosity of Water. The values of ${\Delta f_n}^{i}$ and ${\Delta D_n}^{i}$ were due to water loading to a bare QCM chip and were highly reproducible (i.e., ${\Delta f_3}^{i}/3 = \sim380$ Hz for more than 200 chips tested), which gave QCM the ability in determining the viscosity of a liquid.[22,26,27] From eqs 15 and 28, we have the following equations for viscosity determination:

$$\eta_L = \frac{\pi(\rho_q v_q \Delta f_{L,n})^2}{n\rho_L {f_{q,1}}^3} = (1.99\times10^{-6})\frac{\Delta f_{L,n}}{\rho_L} \quad (34)$$

$$\eta_L = \frac{n\pi(\rho_q v_q \Delta D_{L,n})^2}{4\rho_L f_{q,1}} = (1.24\times10^{4})\frac{\Delta D_{L,n}}{\rho_L} \quad (35)$$

where $\Delta f_{L,n} = {\Delta f_n}^{i}$, $\Delta D_{L,n} = {\Delta D_n}^{i}$.

In this study, both ${\Delta f_n}^{i}$ and ${\Delta D_n}^{i}$ were first applied, as an internal control, to extract the viscosity of water (see Supporting Information Figure S3). The calculated values (8.9×10^{-4} and 9.1×10^{-4} N s m^{-2} from ${\Delta f_n}^{i}$ and ${\Delta D_n}^{i}$, respectively) agreed well with the literature value (8.9×10^{-4} N s m^{-2}). Equations 34 and 35 were applicable to measure the viscosity of other solutions.

Density of Dry and Wet Films. Lu et al. developed an equation similar to that of eq 5 and proved that the Sauerbery equation was only a special case of their model.[28] Equation 32 became eq 5 when there was no liquid loading because ${\Delta f_n}^{iii} = \Delta f_{L,n}$, indicating both Sauerbery and Lu's equations were special cases of eq 32. From eqs 5 and 32, one has

$$\rho_{f,dry} = \frac{k_{2,dry}}{5.60\times10^{-3}} \quad (36)$$

where $k_{2,dry}$ was experimentally determined (Figure 3B and Figure S7).

The values of $\rho_{f,dry}$ were thus extracted from eq 36 as listed in Table 2, which made QCM (not necessary QCM-D in this case) a simple yet effective tool in determining the surface density of ultrathin polymer brushes at dry state under ambient environment (not necessary under high vacuum condition). We identified a linear $f-t$ relation up to 150 nm for QCM-D operating under ambient atmosphere (Figure S7), although the values of $k_{2,dry}$ were different (7.64 for films less than 30 nm and 6.55 for films up to 150 nm with a corresponding $\rho_{f,dry}$ at 1170 kg m^{-3}). The initiator density had minor impact on the value of $\rho_{f,dry}$ (Table 2), which could be explained by the fact that density difference was minimized after films were collapsed.

One must not confuse $k_{2,dry}$ with $k_{2,n}$. These two values were different only by a factor of $\rho_{f,dry}$ or $\rho_{f,wet}$, but the direct measurement of $\rho_{f,wet}$ (therefore $k_{2,n}$) was not possible in the current QCM-D experiments. However, we have ${\Delta f_n}^{ii} = \Delta f_{f,n} + \Delta f_{f,L,n}$ from the experimental design. Substituting eqs 17, 32 and 33 to eq 4, we have eq 37 (see Supporting Information for details, eqs S7−S13):

$$\rho_{f,wet} = 89.3\left(k_{1,n,a} + \frac{4.99\times10^{-3}}{6.4\times10^{-11}}\frac{\eta_0}{\mu_0}n^{(d-c)2}k_{D,n,a}\right) \quad (37)$$

The calculated $\rho_{f,wet}$ values (Table 2) were unreasonably high for polymeric materials. The QCM was only able to detect the area averaged mass ($\rho_{f,water}d$). In order to obtain accurate thickness information, independent determination of thickness was required, and vice versa. Due to technical difficulties in determining the value of $\rho_{f,wet}$, common practice was to estimate $\rho_{f,wet}$ based on the fractions of component density.[10,19,22] Martin et al. theoretically predicted that liquid trapped in polymers could be treated as solid.[29] On the basis of this prediction, we hypothesized that poly(OEGMA) brushes vibrating at high frequency acted as a rigid container. And water filled into this container became a part of the vibrating rigid material. Assuming that d' was the amount of water needed to swell the polymer brush from thickness d (i.e., the dry film thickness) to Rd (i.e., the wet film thickness, $R = t_{f,wet}/t_{f,dry}$), we calculated the density as $\rho_{f,wet} = (\rho_{f,dry}d + \rho_{f,water}d')/(Rd)$. Thus, the density was determined by the values of R and d'. Since the volume of water will expand when it dissolves solutes, we have $d' \le (Rd)$. Thus, for a fixed R value, the maximum $\rho_{f,wet}$ was $(\rho_{f,dry} + \rho_{f,water})/R$. If applying the optical thickness, we had $R = 2$ and the maximum $\rho_{f,wet} = (1364 + 1000)/2 = 1182$ kg m^{-3}, which was much smaller than the value of 1770 kg m^{-3} calculated from eq 37 for 1.00 initiator density (Table 2). If applying the acoustic thickness, we had $R = 4$ and the calculated density $\rho_{f,wet} = 883$ kg m^{-3} (Tables S3 and S4), which was larger than the value of $(1364 + 1000)/4 = 591$ kg m^{-3}, indicating $d' > 4d$ (i.e., the volume of water shrinks when it dissolves poly(OEGMA)). Neither the optical thickness nor the acoustic thickness provided a satisfactory solution to this thickness and density conflict. A separate paper will be dedicated

(26) Kanazawa, K. K.; Gordon, J. G., II *Anal. Chem.* **1985**, *57*, 1770.
(27) Borovikov, A. P. *Instrum. Exp. Tech.* **1976**, *19*(1), 223–224.
(28) Lu, C. In *Methods and Phenomena—Their Applications in Science and Technology*; Lu, C., Czanderna, A. W., Eds.; Elsevier: New York, 1984; pp 393.
(29) Martin, S. J.; Frye, G. C.; Ricco, A. J.; Senturia, S. D. *Anal. Chem.* **1993**, *65*, 2910.

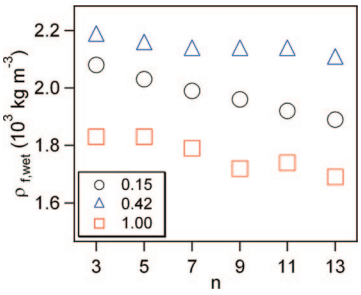

Figure 6. Overtone-dependent frequency changes reveal wet film density of poly(OEGMA) brushes. The values of $\rho_{f,wet}$ for three tested initiator densities, namely, 1.00, 0.42, and 0.15, were plotted against n.

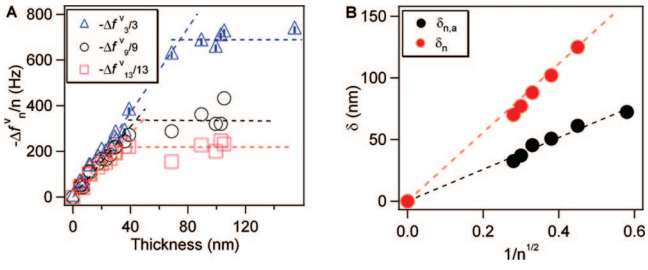

Figure 7. The penetration depth. (A) $k_{1,n,a}$ at different overtones, for clarity only shown are $n = 3$, 9, 13. The viscous penetration depth δ_n of the thickness−shear wave was determined from the intersection of two lines. (B) Values of δ_n and $\delta_{n,a}$ at six overtones were plotted against $1/n^{1/2}$, $R^2 = 0.99$. The error bar for thickness was marked in Δf^{ii} and was the same for all n.

to address this conflict and compare the dissipation method (i.e., QCM-D) with the impedance method by converting the dissipation factor to impedance.

Other Implications. We have only analyzed films of thickness up to 30 nm. Although the linear relation for dry film as indicated by eq 5 held up to 150 nm (Figure S7), this was not the case for wet film. The working range for eq 4 was much shorter than 150 nm. The linear relation held up to a certain thickness until a plateau appeared for Δf_n^{ii} (Figure 7A for 1.00 initiator density). This critical thickness was n dependent and was related to the penetration depth of the thickness−shear wave of a vibrating QCM chip. We applied a simplified physical model for wave propagation. This model assumed the wave propagated without any decay and suddenly became zero at the critical thickness, as defined by the intersection of two lines for a fixed n value. The so obtained $\delta_{n,a}$ values (the subscript n indicated δ was overtone number dependent and a was abbreviated for apparent) were plotted against $1/n^{1/2}$, and a linear fit was obvious as theoretically predicated by eqs 9, 38, and 39 (Figure 7B), giving $k_{\delta,a} = 1.29 \times 10^{-7}$:

$$\delta_n = k_\delta \sqrt{\frac{1}{n}} \tag{38}$$

$$k_\delta = \sqrt{\frac{\eta_f}{(1.56\times 10^7)\rho_{f,wet}}} \tag{39}$$

Note that the so determined $k_{\delta,a}$ was for dry film thickness. Since both η_f and $\rho_{f,wet}$ for wet films were calculated using $R = t_{f,wet}/t_{f,dry} \approx 2$, the values of δ_n and k_δ from eqs 38 and 39 should reflect this 2-fold increase. It was confirmed by Figure 7B that the calculated values of δ_n and k_δ (2.78×10^{-7}) were about 2 times higher than those experimentally determined values. If the impact of vibration amplitude on the thickness−shear wave and its decay behavior can be physically described in a more rigorous model,[30,31] δ_n can be precisely defined by experiments and therefore omit the need of $R_{wet/dry}$ determination. One important observation was that the linear relation had a larger working range for small overtone number, an important rule for experimental design where a linear relation was desired.

Table 3. List of Calculated k Values for Poly(OEGMA) at 1.00 Initiator Densities

N	$k_{1,n}{}^a$	$k_{2,n}{}^b$	$k_{3,n}{}^c$
3	9.14	10.37	1.24
5	9.03	10.40	1.38
7	8.64	10.20	1.56
9	8.14	9.80	1.66
11	8.19	9.97	1.78
13	7.80	9.69	1.89

[a] $k_{1,n} = k_{1,n,a}/R$ ($R = t_{f,wet}/t_{f,dry} \approx 2$). [b] $k_{2,n} = k_{1,n} + k_{3,n}$. [c] Calculated according eq 33. See Tables S5 and S6 for 0.42 and 0.15 initiator densities.

The fact that one can subtract Δf^i from Δf^{iv} for any polymer-coated surfaces (see eqs 1 and 34 and Figure S3) implied that the surface morphology did not impose significant impact on the Δf^i value, or very unlikely that the polymer brush did not change the morphology of the QCM chip. From Scheme 1A, we were unable to design an experiment that can single out the value of $\Delta f_{f,n}$. Instead, one measured the value of Δf^{iii}, which was the frequency change solely due to mass increase. The value of Δf^{iv} thus contained frequency change due to partial mass change (the difference between $\rho_{f,dry}$ and $\rho_{f,wet}$) and viscoelastic damping ($\Delta f_{f,L,n}$). From Table 3, it was clear that viscoelasticity contributed only a small portion of the frequency change. Therefore, it was reasonable to use $k_{1,n}$ as an indication of wet mass increase, which was important for QCM-D application as a biosensor.

Conclusion

In conclusion, this coupled QCM-D and ellipsometry study of ultrathin poly(OEGMA) brushes provided a set of equations, either empirical or based on the Voigt model, that were useful as indicated below: (i) empirical equations (3)−(6) revealed the linear $f-t/D-t$ relations and were the basis for further calculations, (ii) eqs 21–25 were for the calculation of η_f and μ_f of poly(OEGMA) brushes, (iii) eqs 34 and 35 were for the calculation of viscosity of solutions, (iv) eqs 36 and 37 revealed $\rho_{f,dry}$ and $\rho_{f,wet}$, respectively, (v) eqs 38 and 39 were useful in experimental design by providing δ, where linear response started to fail (working range for the aforementioned empirical equations).

QCM-D was invented 12 years ago[11] and theoretical prediction of the possibility in measuring viscoelasticity was made 8 years ago.[12] We realized such measurement because of the application of SIP, which enabled us to control the brush thickness in steps of a few nanometers. The significance of a clear physical description of viscoelasticity of ultrathin polymer brushes lies on not only the fundamental aspects of polymeric materials at nanometer length scale but also related important physiological behaviors. In forthcoming publications, we will demonstrate the application of these equations and extracted physical properties in studying the process of SIP (empirical eqs 3–6 were key to the kinetic study of SIP) and realizing QCM-D as a biosensor.

Acknowledgment. We thank Dr. G. Jin for help with ellipsometry modeling, Dr. F. Yuan and Dr. D. Johannsmann for help with the Voigt model. This project was supported by NSFC grants (20644001, 20604002) and a NSFB grant (2072008) to H.M.

(30) Du, B. Y.; Johannsmann, D. *Langmuir* **2004**, *20*, 2809.
(31) Johannsmann, D.; Heim, L. O. *J. Appl. Phys.* **2006**, *100*, 094505.

Supporting Information Available: Figures showing vacuum drying is not necessary, the optical constant A_n in the Cauchy model has minimal impact on $t_{f,dry}$, the viscosity of water can be measured and $\Delta f^i/\Delta D^i$ is reproducible, the relationship between dissipation/frequency and thickness changes, calculated viscoelasticity properties, and the $k_{2,dry}$ value is independent of thickness and initiator density, tables showing variation of absolute frequency values due to reloading of chips, calculated viscoelasticity, lists of fitted values, viscoelastic properties, and calculated density values for poly(OEGMA) at different initiator densities, and lists of calculated k values for poly(OEGMA) at different initiator densities, and deduction of equations for $\rho_{wet,f}$. This material is available free of charge via the Internet at http://pubs.acs.org.

LA703661Z